Journal of Physics B: Atomic, Molecular and Optical Physics

PAPER • **OPEN ACCESS**

Three-octave terahertz pulses from optical rectification of 20 fs, 1 μm, 78 MHz pulses in GaP

To cite this article: Jia Xu *et al* 2018 *J. Phys. B: At. Mol. Opt. Phys.* **51** 154002

OPEN ACCESS
IOP Publishing
Journal of Physics B: Atomic, Molecular and Optical Physics
J. Phys. B: At. Mol. Opt. Phys. **51** (2018) 154002 (5pp)
https://doi.org/10.1088/1361-6455/aacfe7

Three-octave terahertz pulses from optical rectification of 20 fs, 1 μm, 78 MHz pulses in GaP

Jia Xu[1], Björn Globisch[2], Christina Hofer[1,3], Nikolai Lilienfein[1,3], Thomas Butler[1], Nicholas Karpowicz[1,3] and Ioachim Pupeza[1,3]

[1] Max-Planck-Institut für Quantenoptik, Hans-Kopfermann-Straße 1, D-85748 Garching, Germany
[2] Fraunhofer-Institut für Nachrichtentechnik, Heinrich-Hertz-Institut, Einsteinufer 37, D-10587 Berlin, Germany
[3] Ludwig-Maximilians-Universität München, Am Coulombwall 1, D-85748 Garching, Germany

E-mail: ioachim.pupeza@mpq.mpg.de

Received 23 February 2018, revised 1 May 2018
Accepted for publication 28 June 2018
Published 10 July 2018

Abstract

We demonstrate optical rectification of 1 μm pulses with a duration of 20 fs, a repetition-rate of 78 MHz and an average power of 5.5 W, in a 2 mm thick GaP crystal. The spectrum of the resulting far-infrared pulses is centered at 1.5 THz and extends to 5 THz at −50 dB intensity. In the absence of resonant absorption of GaP in this range, the spectrum has a well-behaved shape, facilitating spectroscopic applications. In the context of the recent rapid evolution of high-power Yb-based femtosecond laser systems, these results show a viable route towards sources of THz pulses combining broad bandwidth, high average power and a smooth spectral shape.

Keywords: terahertz spectroscopy, ultrafast lasers, ultrafast nonlinear optics

(Some figures may appear in colour only in the online journal)

1. Introduction

The generation of coherent THz transients and the possibility to sample their electric fields—both processes using ultrashort near-infrared (NIR) laser pulses—have marked the birth of THz time-domain spectroscopy (THz-TDS) about three decades ago [1, 2]. Since then, the coherent nature of this scheme, rendering it insensitive to thermal background and enabling the detection of very weak fields, has led to a rapid growth of the fields of THz spectroscopy and microscopy. Today, THz-TDS is widely employed in areas including non-destructive inspection, gas sensing, biological research and material science, to name a few examples [3–7]. The steadily increasing number of applications is accompanied by a growing demand for THz-TDS systems combing broadband spectral coverage with high average power and, preferably, a high-repetition-rate.

There are three main, well-established methods for ultrafast-laser-based THz generation and detection: laser-driven gas ionization [8–12], photoconductive switching in semiconductor-based antennas [13–18] and phase-matched optical rectification (OR) in crystals [19–23]. The first method relies on the ionization of gas atoms/molecules, leading to a current of photoelectrons with a steep temporal gradient [10, 11]. While with this method, ultrabroadband THz spectra reaching deep in the mid-infrared range have been generated [9, 12], photoionization of the gas requires peak intensities of the driving laser field on the order of 10^{13}–10^{15} W cm^{-2}. Such intensities are usually available only at repetition rates significantly below 1 MHz, limiting the average power of driving laser systems to the Watt level. Together with conversion efficiencies in the range of 10^{-6}–10^{-3}, this results in at most a few hundreds of μW of THz average powers [12].

Generation and detection of THz radiation using photoconductive antennas (PCAs) has been extensively studied after the first demonstration by Auston and Smith in 1983

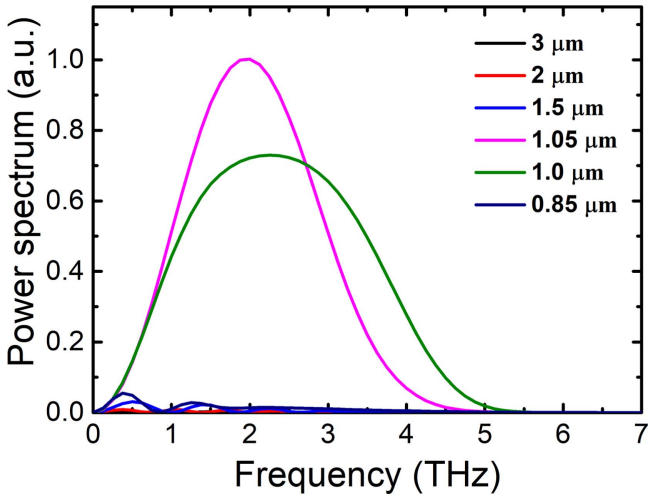

Figure 1. Simulations of OR in a 2 mm GaP crystal, driven by 20 fs pulses with different central wavelengths, as indicated in the legend. The highest-efficiency broadband phase-matching can be achieved with driving pulses around 1 μm. The theoretical model is described in section 3.

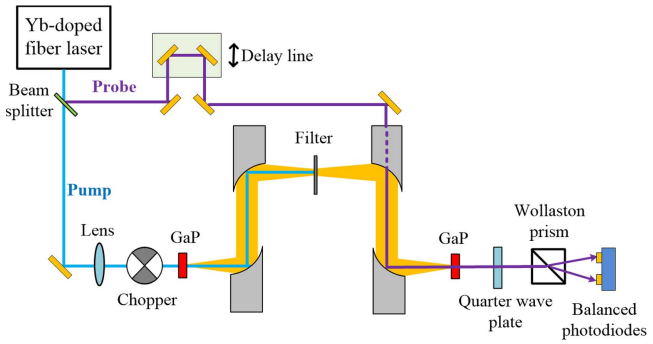

Figure 2. Schematic diagram of the experimental setup for THz generation and detection. The blue and purple lines represent the pump and probe beam paths, respectively. The yellow beam represents the path of the THz pulses.

[13], in particular with titanium-sapphire and erbium-doped fiber lasers. In 2003, Shen *et al* reported the generation and detection of THz radiation by using low-temperature-grown GaAs PCAs driven with a 12 fs titanium-sapphire laser, resulting in frequencies beyond 30 THz at −60 dB intensity [14], albeit suffering from the poor power scalability inherent to this laser technology. The central wavelength of erbium-doped fiber lasers coincides with the minimum absorption in fused silica, providing ideal conditions for fiber-coupled PCAs, employing pulse durations around 100 fs for generation and detection [16]. While these systems reach impressive peak dynamic ranges of more than 100 dB, allowing the detection of frequency components up to 5 THz, the −30 dB spectral width is currently limited to 2.5 THz, with a THz average power of up to 100 μW, at 120 V bias voltage and 30 mW illumination power [16]. THz generation with PCAs driven by 1.0 μm lasers [17, 18] has so far not surpassed these parameters.

The second-order nonlinear process of OR has been used in conjunction with a multitude of nonlinear crystals and driving wavelengths. High pulse energies (>100 μJ) were achieved by OR in $LiNbO_3$ using the tilted pulse front scheme and cryogenically cooled crystals, but the spectral emission is confined to 0.1–1 THz at −20 dB intensity [19, 20]. Organic THz crystals, such as DAST [21], DSTMS [22], HMQ-TMS [23] can offer 10 THz broad spectra at room temperature. However, strong transverse optical (TO) phonon resonances at multiple THz frequencies [24] have several detrimental effects. Firstly, they limit the power scalability due to strong absorption [25]. Secondly, the strong absorption renders accurate spectroscopic measurements around these frequencies challenging. As an indirect bandgap zincblende crystal, GaP has a moderate electro-optic coefficient ($d_{14} = 70.6$ pmV^{-1} at 1.064 μm) and its first TO phonon frequency is lying as high as 11 THz, which potentially affords a smooth frequency response in the <10 THz range [26].

Figure 1 shows calculated OR spectra for 20 fs driving pulses and a 2 mm thick GaP crystal. An optimum with respect to the bandwidth and efficiency is reached for driving wavelengths around 1 μm. In addition, the absorption coefficients of GaP single crystals are low in both the THz wave ($\alpha \sim 3$ cm^{-1} at 1 THz) and NIR ranges ($\alpha < 0.1$ cm^{-1} at 1.064 μm). In particular, in the context of the rapidly progressing Yb-based high average-power laser technology [27–34], these aspects make OR of ultrashort ~1 μm pulses in GaP a highly promising route towards the combination of high THz average power and broad bandwidth. So far, Chang *et al* reported THz generation in GaP pumped by a 210 fs, 10 W Yb-fiber laser, providing 6.5 μW average power with a −60 dB spectral width of 3.5 THz [35]. Li *et al* showed THz pulse generation in GaP driven with a chirp-tunable sub-60 fs Yb-fiber amplifier and an average power of 82.6 μW was obtained at 9 W pump power with negatively chirped pulses, at the cost of THz spectral bandwidth (2 THz at −10 dB intensity) [36].

In this work, we investigate the bandwidth scaling of OR in GaP, driven by ultrafast pulses spectrally centered at 1.05 μm. With a 78 MHz-repetition-rate train of 20 fs pulses with an average power of 5.5 W, we generated and detected a three-octave-spanning THz spectrum, centered at 1.5 THz and extending to 5 THz at −50 dB intensity, via OR in a 2 mm thick (110) GaP crystal. To the best of our knowledge, this is the broadest THz spectrum generated with a 1.0 μm, MHz-repetition-rate ultrafast pump source. Furthermore, the scheme is likely to be power scalable and the well-behaved shape of the spectrum is beneficial for applications in spectroscopy.

2. Experimental setup

Figure 2 shows the experimental setup for THz generation and field-resolved detection. The pump source is an Ytterbium-based master-oscillator-power-amplifier laser system. The Yb:KYW seeding oscillator delivers 170 fs pulses with an average power of 220 mW at a repetition frequency of

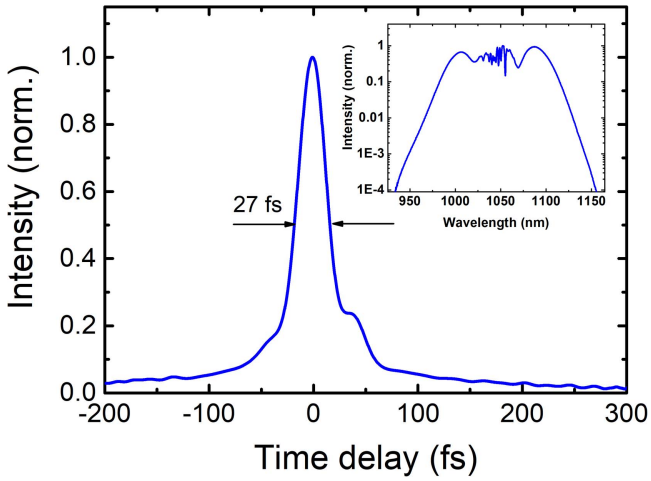

Figure 3. Measured autocorrelation trace. Inset: measured optical spectrum of the 1 μm driving pulses.

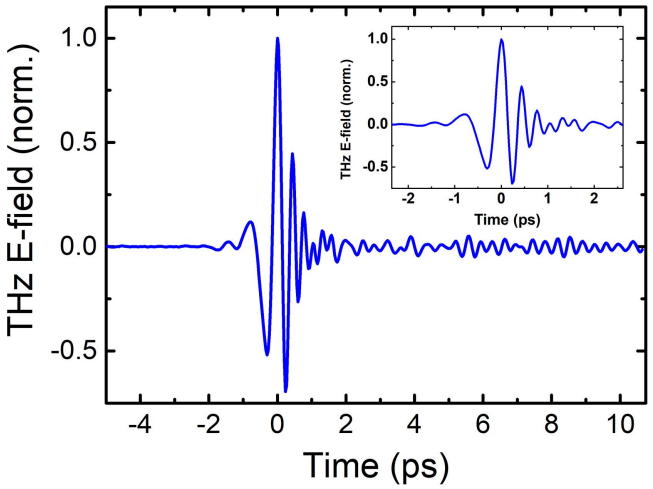

Figure 4. THz transient electric field generated by optical rectification in a 2 mm thick GaP crystal and detected by electro-optic sampling. Inset: zoomed in time window.

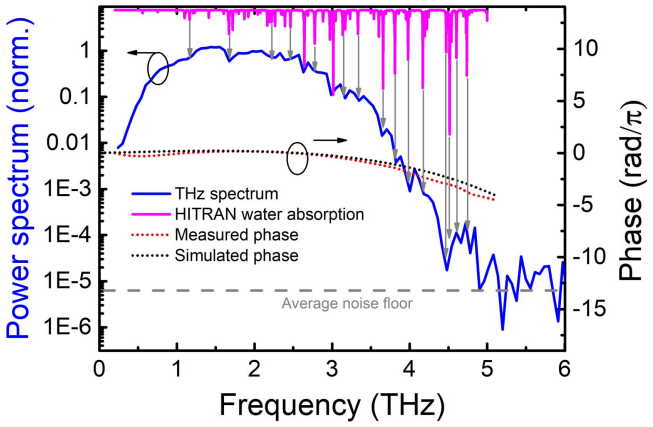

Figure 5. Blue line: power spectrum of the THz wave calculated by Fourier transform. Pink line: water absorption lines from HITRAN database. Red dots: spectral phase calculated by Fourier transform of the EOS time-domain trace. Black dots: simulated spectral phase of THz beam transmitted through 2 mm thick GaP crystal.

78 MHz. The pulses are amplified using a chirped-pulse amplifier (CPA) with a transmission-grating-based stretcher and compressor, and a two-stage fiber amplifier [31]. The output of the CPA is a train of 270 fs pulses which is launched to a large-mode-area photonic crystal fiber (LMA-25, NKT) for spectral broadening. Subsequent compression to a pulse duration of 20 fs is achieved with chirped mirrors. The maximum output power is 11 W. The spectrum and auto-correlation are shown in figure 3.

The 20 fs pulses are split into a pump beam (5.5 W) for THz generation and a probe beam (400 mW) for detection. The pump beam is focused by a lens with 250 mm focal length into a 2 mm thick (110) GaP crystal (Egorov Scientific). The THz pulses are generated in transmission geometry by OR. The following four 90° off-axis parabolic mirrors are used to collect, collimate and focus the THz radiation for electro-optical detection. The probe beam is guided over a delay line and superimposed onto the THz beam through the hole in the third parabolic mirror. The THz beam and probe beams are focused on a 500 μm thick (110) GaP crystal for standard electro-optic sampling [37–39]. The pump beam is modulated by a mechanical chopper, operating at 3.8 kHz, and the signal is read out by a lock-in amplifier with 300 ms time constant. The output power of the THz wave is measured by a Golay cell (TYDEX). The entire setup is enclosed and purged with dry nitrogen to reduce water vapor absorption. The humidity was approximately 15% during all measurements.

3. Results and analysis

Broadband THz radiation is generated by OR in a 2 mm thick GaP crystal at an optical pump power of 5.5 W. The beam diameter on the GaP crystal is around 80 μm, and the peak intensity is 70 GW cm^{-2}, which is close to the damage threshold of GaP reported in [40]. The average power of the THz wave is 1.5 μW measured by a commercial Golay cell, which is comparable to the results in [35]. A black painted ceramic filter is used to block the residual IR beam. The transmission of this filter is measured to be ~70% in the THz range. Figure 4 shows the measured THz transient electric field. The THz pulse duration determined from these data is ~570 fs (intensity FWHM). The main pulse is followed by a series of oscillations extending to 10 ps, originating from water vapor absorption. Figure 5 shows the corresponding THz power spectrum and spectral phase calculated by Fourier transform. The THz spectrum is centered at 1.5 THz and extends to more than 5 THz with a 55 dB detection dynamic range. The dips in the spectrum stem from residual water vapor absorption along the THz wave path, as confirmed by comparison with the water absorption lines (plotted in pink line) from the HITRAN database [41]. The simulated spectral phase is calculated from the refractive index of GaP [42], taking into account the thickness of the crystal. The measured and simulated phase show excellent agreement. The spectral phase is almost flat for frequencies lower than 2 THz. Since GaP has a strong resonant TO phonon peak around 11 THz

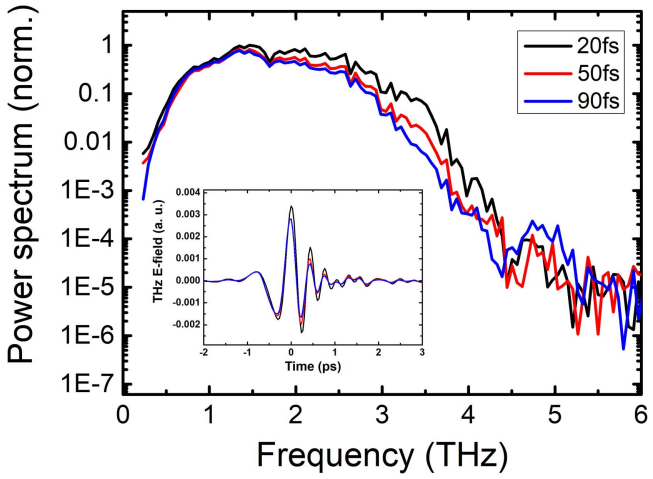

Figure 6. THz spectrum generated in 2 mm thick GaP crystal by using 20, 50 and 90 fs pulses. Inset: the corresponding THz transient electric field.

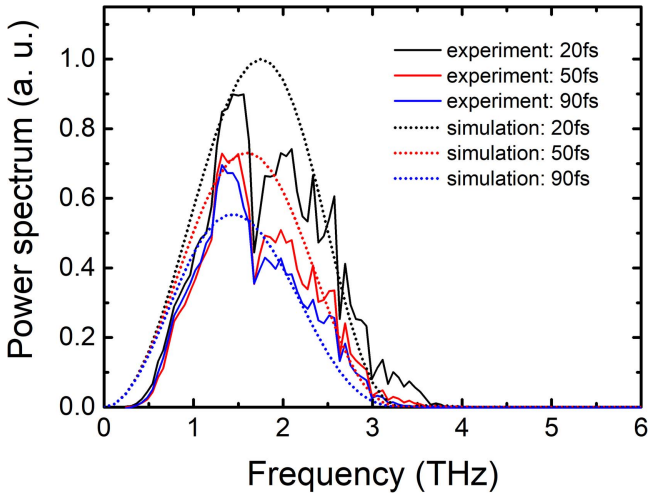

Figure 7. Simulated and experimental THz spectra with 20, 50 and 90 fs pulses. The spectra are normalized at 1.4 THz, in a region unaffected by water vapor absorption.

[42], the material dispersion is relatively large in the THz range of a few THz, leading to a visible chirp on the pulse.

By tuning the grating pair inside the Yb CPA system, the duration of the driving pulses is altered to 50 fs and 90 fs, respectively. Driving OR with longer pulses results in a significant decrease of the THz power spectral density at higher frequencies, as illustrated in figure 6.

To confirm the results theoretically, we carried out simulations of the THz generation and detection processes. The simulations are based on the nonlinear wave equation in the slowly-varying amplitude approximation, and account for the full dispersion and nonlinear propagation of broadband light pulses. The governing differential equation in the frequency domain reads [43]:

$$\frac{\partial E_\omega(z)}{\partial z} = -ik_\omega E_\omega(z) - \frac{i\omega}{2n(\omega)\varepsilon_o c} P_\omega^{(NL)}(z), \qquad (1)$$

where E_ω is the complex amplitude of an individual spectral component, $P_\omega^{(NL)}$ is the nonlinear polarization (here governed by a second-order susceptibility), and n(ω) is the frequency-dependent refractive index [37]. In figure 7, the simulated and detected spectra are compared, showing very good agreement when phase-matching and NIR-pulse-dependence of both OR and EOS are considered.

4. Conclusion

In summary, we have presented broadband THz generation by OR of 20 fs pulses spectrally centered at 1 μm, with an average power of 5.5 W and a repetition frequency of 78 MHz, in a GaP crystal. With electro-optical sampling employing a 0.5 mm GaP crystal, frequencies up to 5 THz (at −50 dB intensity) are measured. To the best of our knowledge, this represents the most broadband THz spectrum generated with Yb-based laser systems. We show in theory and experiment that the short pulse duration is crucial for achieving this bandwidth. The power level in the few-μW range is consistent with previous experiments. Given the power scalability of OR in GaP [35, 36] and the recent progress towards high-power Yb-based lasers [27–34], these results show a viable route towards the generation of high-power, broadband, high-repetition-rate THz pulses.

Acknowledgments

We acknowledge support of the 'Fiber and Waveguide Lasers' group at the Institute of Applied Physics of the University of Jena and we thank Ferenc Krausz for helpful discussions.

ORCID iDs

Jia Xu https://orcid.org/0000-0003-2260-8554

References

[1] Wu Q and Zhang X C 1995 Free-space electro-optic sampling of terahertz beams *Appl. Phys. Lett.* **67** 3523
[2] Smith P R, Auston D H and Nuss M C 1998 Subpicosecond photoconducting dipole antennas *IEEE J. Sel. Top. Quantum Electron.* **24** 255
[3] Tonouchi M 2007 Cutting-edge terahertz technology *Nat. Photon.* **1** 97–105
[4] Hafez H A, Chai X, Ibrahim A, Mondal S, Férachou D, Ropagnol X and Ozaki T 2016 Intense terahertz radiation and their applications *J. Opt.* **18** 093004
[5] Dhillon S S *et al* 2017 The 2017 terahertz science and technology roadmap *J. Phys. D: Appl. Phys.* **50** 043001
[6] Yang X, Zhao X, Yang K, Liu Y, Liu Y, Fu W and Luo Y 2016 Biomedical applications of terahertz spectroscopy and imaging *Trends Biotechnol.* **34** 810–24
[7] Jepsen P U, Cooke D G and Koch M 2011 Terahertz spectroscopy and imaging—modern techniques and applications *Laser Photonics Rev.* **5** 124–66

[8] Cook D J and Hochstrasser R M 2000 Intense terahertz pulses by four-wave rectification in air *Opt. Lett.* **25** 1210–2

[9] Kim K Y, Taylor A J, Glownia J H and Rodriguez G 2008 Coherent control of terahertz supercontinuum generation in ultrafast laser-gas interactions *Nat. Photon.* **2** 605–9

[10] Karpowicz N, Lu X and Zhang X C 2009 Terahertz gas photonics *J. Mod. Opt.* **56** 1137–50

[11] Dai J, Clough B, Ho C, Lu X, Liu J and Zhang X C 2011 Recent progresses in terahertz wave air photonics *IEEE Trans. Terahertz Sci. Technol.* **1** 274–81

[12] Thomson M D, Blank V and Roskos H G 2010 Terahertz white-light pulses from an air plasma photo-induced by incommensurate two-color optical fields *Opt. Express* **18** 23173–82

[13] Auston D H and Smith P R 1983 Generation and detection of millimeter waves by picosecond photoconductivity *Appl. Phys. Lett.* **43** 631–3

[14] Shen Y C, Upadhya P C, Linfield E H and Beere H E 2003 Ultrabroadband terahertz radiation from low-temperature-grown GaAs photoconductive emitters *Appl. Phys. Lett.* **83** 3117–9

[15] Hale P J, Madeo J, Chin C, Dhillon S S, Mangeney J, Tignon J and Dani K M 2014 20 THz broadband generation using semi-insulating GaAs interdigitated photoconductive antennas *Opt. Express* **22** 26358–64

[16] Globisch B, Dietz R J B, Göbel T, Schell M, Bohmeyer W, Müller R and Steiger A 2015 Absolute terahertz power measurement of a time-domain spectroscopy system *Opt. Lett.* **40** 3544–7

[17] Dietz R J B *et al* 2013 Low temperature grown Be-doped InGaAs/InAlAs photoconductive antennas excited at 1030 nm *J. Infrared, Millim., Terahertz Waves* **34** 231–7

[18] Kong M S, Kim J S, Han S P, Kim N, Moon K, Park K H and Jeon M Y 2016 Terahertz radiation using log-spiral-based low-temperature-grown InGaAs photoconductive antenna pumped by mode-locked Yb-doped fiber laser *Opt. Express* **24** 7037–45

[19] Fülöp J A, Pálfalvi L, Klingebiel S, Almási G, Krausz F, Karsch S and Hebling J 2012 Generation of sub-mJ terahertz pulses by optical rectification *Opt. Lett.* **37** 557–9

[20] Vicario C, Monoszlai B, Lombosi C, Mareczko A, Courjaud A, Fülöp J A and Hauri C P 2013 Pump pulse width and temperature effects in lithium niobate for efficient THz generation *Opt. Lett.* **38** 5373–6

[21] McLaughlin C V, Hayden L M, Polishak B, Huang S, Luo J, Kim T D and Jen A K Y 2008 Wideband 15 THz response using organic electro-optic polymer emitter-sensor pairs at telecommunication wavelengths *Appl. Phys. Lett.* **92** 151107

[22] Jeong J H *et al* 2016 A broadband THz-TDS system based on DSTMS emitter and LTG InGaAs/InAlAs photoconductive antenna detector *Sci. Rep.* **6** 26949

[23] Rovere A, Jeong Y G, Piccoli R, Lee S H, Kwon O P, Jazbinsek M, Morandotti R and Razzari L 2018 Generation of high-field terahertz pulses in an HMQ-TMS organic crystal pumped by an ytterbium laser at 1030 nm *Opt. Express* **26** 2509–16

[24] Cunningham P D and Hayden L M 2010 Optical properties of DAST in the THz range *Opt. Express* **18** 23620–5

[25] Cao L, Teng B, Xu D, Zhao H, Lun H, Yao J and Guo J 2016 Growth, transmission, Raman spectrum and THz generation of DAST crystal *RSC Adv.* **6** 101389–94

[26] Wu Q and Zhang X C 1996 Design and characterization of traveling-wave electrooptic terahertz sensors *IEEE J. Sel. Top. Quantum Electron.* **2** 693–700

[27] Jauregui C, Limpert J and Tünnermann A 2013 High-power fibre lasers *Nat. Photon.* **7** 861

[28] Russbueldt P *et al* 2015 Innoslab amplifiers *IEEE J. Sel. Top. Quantum Electron.* **21** 447–63

[29] Pronin O, Seidel M, Lücking F, Brons J, Fedulova E, Trubestskov M, Pervak V, Apolonski A, Udem T and Krausz F 2015 High-power multi-megahertz source of waveform-stabilized few-cycle light *Nat. Commun.* **6** 6988

[30] Saule T, Holzberger S, De Vries O, Plötner M, Limpert J, Tünnermann A and Pupeza I 2017 Phase-stable, multi-μJ femtosecond pulses from a repetition-rate tuneable Ti:Sa-oscillator seeded Yb-fiber amplifier *Appl. Phys.* B **123** 17

[31] Eidam T, Röser F, Schmidt O, Limpert J and Tünnermann A 2008 57 W, 27 fs pulses from a fiber laser system using nonlinear compression *Appl. Phys.* B **92** 9

[32] Mak K F, Seidel M, Pronin O, Frosz M H, Abdolvand A, Pervak V, Apolonski A, Krausz F, Travers J C and Russell P J 2015 Compressing μJ-level pulses from 250 fs to sub-10 fs at 38 MHz repetition rate using two gas-filled hollow-core photonic crystal fiber stages *Opt. Lett.* **40** 1238

[33] Hädrich S, Krebs M, Hoffmann A, Klenke A, Rothhardt J, Limpert J and Tünnermann A 2015 Exploring new avenues in high repetition rate table-top coherent extreme ultraviolet sources *Light Sci. Appl.* **4** 320

[34] Saraceno C J, Emaury F, Heckl O H, Baer C R E, Hoffmann M, Schriber C, Golling M, Südmeyer T and Keller U 2012 275 W average output power from a femtosecond thin disk oscillator operated in a vacuum environment *Opt. Express* **20** 23535–41

[35] Chang G, Divin C J, Liu C, Williamson S L, Galvanauskas A and Norris T B 2006 Power scalable compact THz system based on an ultrafast Yb-doped fiber amplifier *Opt. Express* **14** 7909–13

[36] Li J *et al* 2014 Efficient terahertz wave generation from GaP crystals pumped by chirp-controlled pulses from femtosecond photonic crystal fiber amplifier *Appl. Phys. Lett.* **104** 031117

[37] Leitenstorfer A, Hunsche S, Shah J, Nuss M C and Knox W H 1999 Detectors and sources for ultrabroadband electro-optic sampling: experiment and theory *Appl. Phys. Lett.* **74** 1516–8

[38] Wu Q and Zhang X C 1997 7 terahertz broadband GaP electro-optic sensor *Appl. Phys. Lett.* **70** 1784–6

[39] Pradarutti B, Matthäus G, Riehemann S, Notni G, Nolte S and Tünnermann A 2008 Highly efficient terahertz electro-optic sampling by material optimization at 1060 nm *Opt. Commun.* **281** 5031–5

[40] Li Y, Liu F, Li Y, Chai L, Xing Q, Hu M and Wang Q 2011 Experimental study on GaP surface damage threshold induced by a high repetition rate femtosecond laser *Appl. Opt.* **50** 1958–62

[41] Gordon I E *et al* 2017 The HITRAN2016 molecular spectroscopic database *J. Quant. Spectrosc. Radiat. Transfer* **203** 3–69

[42] Edward D 1997 *Palik, Handbook of Otpical Constants of Solids* (Burlington: Academic) p 450

[43] Keiber S, Sederberg S, Schwarz A, Trubetskov M, Pervak V, Krausz F and Karpowicz N 2016 Electro-optic sampling of near-infrared waveforms *Nat. Photon.* **10** 159–62